

Selected Topics in Rapidity Gap Physics

Jeffrey R. Forshaw
 Department of Physics & Astronomy
 University of Manchester.
 Manchester. M13 9PL.
 UK.

Summary. This talk¹ will review selected topics in rapidity gap physics. In particular I will discuss diffractive jet production and the possibility of searching for the higgs boson using diffraction at the LHC; the dipole picture of diffraction and saturation; and those processes where a large momentum is transferred across the rapidity gap, for which there has been recent progress both experimentally and theoretically.

1 Introduction

Over the past 10 years, due in no small part to the quality and extent of data collected at the HERA and Tevatron colliders, the field of rapidity gap physics has flourished. As a result, in a review talk like this I cannot hope to cover anything other than a few topics, chosen to reflect my personal bias.

The next section will focus on the hard diffractive production of jets and higgs bosons, and will draw on data collected at both HERA and the Tevatron. In Section 3, I discuss the dipole model of diffraction and the evidence for saturation. In Section 4, I turn to rapidity gaps with a large momentum transfer across the gap. These are rarer but rather clean processes, and recent high quality data on vector meson production has allowed comparison with theory, which I discuss.

2 Hard diffraction

I will follow the conventional language and classify hard diffractive processes as shown in Figure 1. Q is some hard scale (e.g. jet transverse momentum, W mass etc.) characteristic of the system X . In “double pomeron exchange”, which has been measured at the Tevatron [1], the protons remain intact, losing only a small fraction of their initial energy, so that the system X is produced centrally. In single diffraction, only one proton remains intact and fast, and the system X is distant from it in rapidity.

¹ Talk presented at the 14th Topical Conference on Hadron Collider Physics, HCP 2002, Karlsruhe, 29 September–4 October 2002.

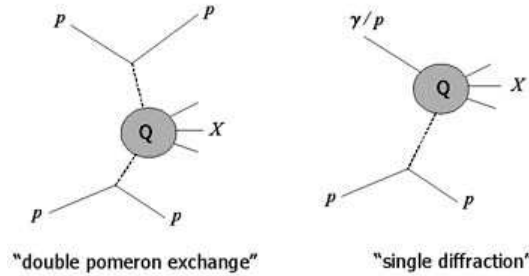


Fig. 1. Hard diffraction

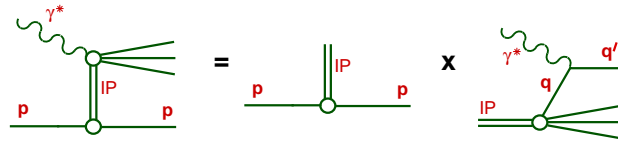


Fig. 2. Regge factorization. (Figure from [4])

At HERA, single diffraction of a virtual photon (virtuality Q^2) has allowed experimenters to probe the partonic structure of the diffractive exchange [2,3]. Appealing to regge theory, one can attempt to write the cross-section as a product of a pomeron flux factor $f_{P/p}$ and a pomeron parton density function, as shown in Figure 2. The experimenters parameterise the flux factor as

$$f_{P/p}(x_P, t) = \frac{e^{Bt}}{x_P^{2\alpha(t)-1}} \quad (1)$$

where x_P is the fraction of the incoming proton's energy carried by the pomeron, t is the momentum transfer to the scattered proton, B is the diffractive slope and $\alpha(t)$ is the pomeron trajectory. The experimenters are able to fit all their data on the diffractive structure function using a parameterisation of this form after evolving the parton density functions using the NLO evolution equations. H1 finds a pomeron intercept $\alpha_P = 1.17 \pm 0.02$ and no need for secondary regge exchanges for $x_P < 0.01$ [5]. H1 has now extracted the pomeron quark and gluon density functions with an estimate of the error, see Fig. 3. Note that it is the gluon at large $z = x/x_P$ which is least well constrained.

If the notion of a universal pomeron parton density function is to be tested, one needs to take the partons as measured in diffractive DIS, and use them to predict the rates for other processes. At HERA this programme has been carried out quite extensively and on the whole there is good agreement [4]. However, there are indications that the DIS partons do tend to lead to an overestimate of the data collected off real photons. Good agreement

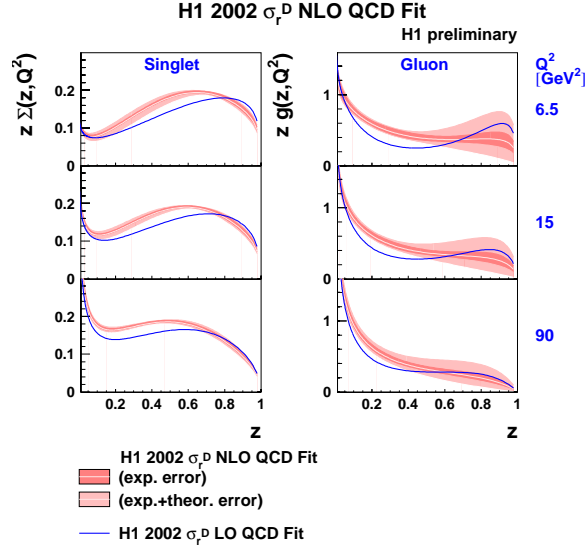


Fig. 3. Pomeron parton density functions extracted by H1 [5]

can be arranged if one is prepared to accept an overall renormalisation by a factor of about 0.6 [6]. Strictly speaking, the need for such a renormalisation violates universality. This should not come as a surprise; we already knew that universality should not hold across the board in diffraction [7]. What would be of interest is if the violation can be understood. Simple (eikonal) models predict that rapidity gaps will be filled in by secondary interactions in those processes where the incoming beam particles have structure, which is the case in hadron-hadron interactions and photon-hadron interactions with an on-shell photon. These simple models also predict that the filling in of gaps can be approximated by an overall multiplicative factor which is weakly process dependent; depending primarily on the overall centre-of-mass energy [8]. In this way we can understand a gap survival factor of ~ 0.6 at HERA. The eikonal models also predict a survival factor of around 0.1 at the Tevatron (the high centre-of-mass energy being the main reason for the reduction since it liberates more low- x partons).

The burning question is therefore: “How does a gap survival factor of 0.1, in conjunction with the latest H1 parton density functions, stand up to the Tevatron data?”. At first sight, the answer is “very badly”. In Table 1, we show the original calculations of [9], which are parton level and do not contain any gap survival factor. Comparison is to CDF and D0 data available at the time (some of which were preliminary). The references shown in the table are to the final published papers. The pomeron parton densities do not now agree with the most recent HERA data, but they are not so far out to

account for the obvious problems. Even with a gap survival of ~ 0.1 , things look bleak.

Table 1. Problems at the Tevatron?

	Experiment	Theory	Theory/Exp.
CDF W [10]	$1.15 \pm 0.51 \pm 0.20\%$	7%	6 ± 3
CDF RG dijet [11]	$0.75 \pm 0.05 \pm 0.09\%$	16%	22 ± 3
CDF pot dijet [12]	$0.109 \pm 0.003 \pm 0.016\%$	4%	34 ± 5
D0 RG dijet [13]	$0.67 \pm 0.05\%$	12%	18 ± 1
CDF heavy quark [14]	$0.18 \pm 0.03\%$	30%	167 ± 28
CDF double pomeron exch. [1]	$13.6 \pm 2.8 \pm 2$ nb	3713 nb	273 ± 69

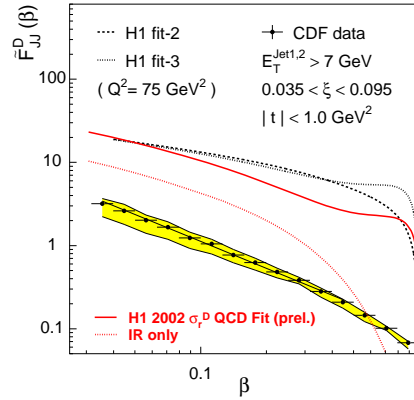


Fig. 4. Comparison of the diffractive dijet rate to CDF data. (Figure from [5])

However, the problem may not be so bad. With the new H1 partons the rate for diffractive dijet production at the Tevatron agrees well with the HERA prediction with a gap survival factor of 0.1. The Tevatron data on diffractive dijet production now go beyond the total rate, as can be seen in Fig. 4 (\tilde{F}_{JJ}^D is a ratio of diffractive to non-diffractive cross-sections and β is the momentum fraction of the parton coming from the pomeron which is involved in the hard subprocess). The solid red curve shows the prediction based on

the latest H1 partons – it agrees in shape with the CDF data, especially once one realises that the large β region is the large z region in Fig. 3 and that the dijet process is gluon dominated. So much for dijet production in single diffraction. What about the double pomeron exchange process (producing central dijets), which is out by two orders of magnitude according to Table 1?

Remarkably even here things seem not to be too bad. Analysis shows that there are large hadronisation corrections to the parton level results of Table 1 which account for a suppression of the theory by a factor of 4 [15]. This suppression comes about because CDF used a small cone $R = 0.7$ to define their central jets, simultaneously with a low E_T cut of 7 GeV. At such low scales the jets are broad and one loses about 2 GeV per jet. In [15], a HERWIG monte carlo simulation of the parton showering and hadronisation [16] was included thereby allowing us to estimate the size of the corrections. In addition, the overall rate is sensitive to the pomeron intercept. A higher intercept leads to a lower cross-section at the Tevatron if the normalisation is fixed at HERA since HERA probes lower values of x_P . The authors of [9] used a soft pomeron intercept which we now know to be inappropriate; this gains another factor of 2. The remaining difference is down to the parton densities in the pomeron. Table 2 summarises the results of [15] where the bottom line shows a difference of a factor 10 between theory and experiment which is in accord with gap survival estimates. Note that there is good reason to expect significant “contamination” from secondary exchanges (\mathbb{R}) in the region of the Tevatron data.

Table 2. Rates for double pomeron exchange: comparison of theory and experiment. Theory calculations performed using H1 fit 3 (LO) partons and the default secondary exchange of [16]

Regge exchange	Parton Level (nb)	Hadron Level (nb)
\mathbb{P}	1175	339
\mathbb{R}	241	58
$\mathbb{P} + \mathbb{R}$	1416	397
CDF data		$43.6 \pm 4.4 \pm 21.6$

2.1 Central higgs production

It has been suggested that the double pomeron exchange process could be utilized at the LHC to produce new particles, in particular the higgs boson [17,18]. If the higgs is produced exclusively, as shown in Fig. 5, then one could

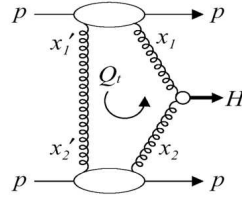


Fig. 5. Exclusive higgs production. (Figure from [18])

reconstruct its mass quite accurately (to within 1 GeV [19]) by tagging the outgoing protons. Moreover, the exclusive nature of the central system leads to a significant suppression of QCD backgrounds, so that one could utilise the $b\bar{b}$ decay of the higgs with a much better S/B compared to the non-diffractive production mechanism. Khoze, Martin and Ryskin (KMS) calculate the rate for the diagram in Fig. 5 and find 3 fb for a 115 GeV higgs decaying to $b\bar{b}$ at the LHC, which should be sufficiently large to permit a good measurement. It is possible to test the reliability of this estimate by performing the corresponding calculation for exclusive central dijet production (i.e. replace the higgs by a dijet pair). KMS predicted a rate of around 1 nb at the Tevatron, which is to be compared to the CDF upper limit of 4 nb [1], i.e. the process has not been seen in Run I data. However, with the increase in data from Run II, and the fact that D0 now has roman pot detectors in both forward and backward directions, it should be possible to check the KMS calculation.

3 Dipole models

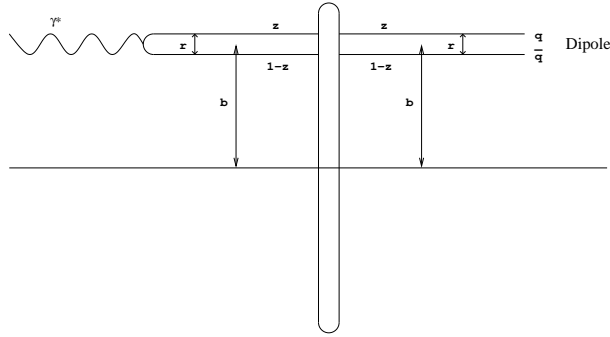


Fig. 6. Diffraction of a colour dipole

Complementary to the regge picture of diffraction in photon induced reactions is the dipole picture, to which we now turn our attention. In the proton rest frame, the incoming photon converts into a $q\bar{q}$ pair a long distance upstream of the proton. In the diffractive limit, the quarks are highly energetic and travel along straight lines through the proton, picking up a non-Abelian phase factor, before eventually forming the diffracted system X way downstream of the proton, see Fig. 6. Consequently, one can write down expressions for a variety of diffractive process, e.g. for the total γp cross-section at high-energy we only need the imaginary part of the forward elastic scattering amplitude, i.e.

$$\sigma_{\gamma p}^{T,L} = \int dz d^2\mathbf{r} |\psi^{T,L}(z, r)|^2 \sigma(s, r, z) \quad (2)$$

where σ is the cross-section for scattering a colour dipole of transverse size r and energy fraction z off a proton. It is universal in that the same dipole cross-section should appear in other processes, such as diffractive vector meson production, where one simply replaces the outgoing photon wavefunction with the meson wavefunction [20]. There is clearly a lot of physics in the dipole cross-section, including the QCD evolution of the original dipole. Apart from the total γp cross-section (and hence the structure functions, F_2 , F_L and F_2^c) and vector meson production, the dipole formalism has been used to compare to data on inclusive diffractive DIS ($F_2^{D(3)}$), deeply virtual Compton scattering and shadowing off nuclei.

In the dipole model of Golec-Biernat & Wüsthoff [21], the dipole cross-section was parameterized as

$$\sigma = \sigma_0 \left\{ 1 - \exp \left(-\frac{r^2}{4R_0(x)^2} \right) \right\} \quad (3)$$

where

$$R_0(x) = \frac{1}{\text{GeV}^2} \left(\frac{x}{x_0} \right)^\lambda$$

and

$$x = \frac{Q^2 + 4m_q^2}{W^2}.$$

$R_0(x)$ is called the saturation radius, since for larger r the cross-section flattens off. Since the saturation radius moves to smaller r as x decreases this model naturally tames the powerlike behaviour of the total cross-section as one moves to smaller x . For small enough r , the cross-section goes like r^2 which generates Bjorken scaling. The striking agreement of the model with data F_2 and on $F_2^{D(3)}$ originally led to the idea that HERA was already probing the non-linear dynamics of saturation. Subsequent, more detailed studies using the latest data, have revealed that it is not possible to fit the data with

a pure power, i.e. λ , which gets tamed by saturation effects. It is necessary to replace the exponent with the gluon density [22], i.e.

$$\sigma = \sigma_0 \left\{ 1 - \exp \left(- \frac{\pi^2 r^2 \alpha_s x g(x)}{3 \sigma_0} \right) \right\}. \quad (4)$$

The gluon density itself becomes less steep as Q^2 falls and so the exponentiation is less important. This means that the regime of large corrections arising from the non-linear dynamics is pushed beyond the HERA region, i.e. to smaller x . The need to go beyond the original model of Golec-Biernat & Wüsthoff is illustrated in Fig. 7 where the effective slope ($\sim x^{-\lambda}$) is shown as a function of Q^2 . In the original model, this slope asymptotes to just below 0.3 and deviations at lower Q^2 are wholly attributed to saturation dynamics. In the new model, there is no flattening at high Q^2 .

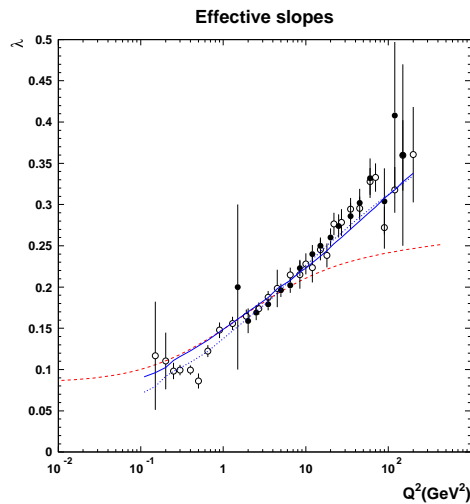


Fig. 7. The effective slope of the low x structure function. Solid curve is the new dipole model, whilst the dashed curve is that from the original Golec-Biernat & Wüsthoff model. (Figure from [22])

A quite different approach can be found in [23]. Here the dipole cross-section is written as a sum of two terms each of which can be thought of as arising from a pure regge pole (of intercepts 1.06 and 1.4 respectively). This “two pomeron” model has no saturation dynamics at all. The reduction of the effective slope at low Q^2 arises because of the dominance of the pomeron with lower intercept in that region (the reverse occurring at high Q^2). This model is also able to describe the available data, including the diffractive structure function $F_2^{D(3)}$ [24] and deeply virtual Compton scattering [25].

Before leaving dipoles, I should say a few things about the latest theoretical progress in the physics of saturation. The use of non-linear perturbative QCD dynamics to control the growth of low- x cross-sections has a long history, dating back to the “GLR equation” of the early 1980’s [26]. More recently, the Balitsky-Kovchegov equation has been developed to describe the non-linear evolution of the S-matrix for scattering a colour dipole off a hadronic target [27]. Underpinning all of this is the colour-glass-dynamics of [28]. Formulated as an effective field theory (analogous to that of glasses in condensed matter physics), the colour glass dynamics describes the quantum evolution of soft gluons in a classical background colour field. It reduces to the BFKL equation in the approximation of a dilute background, and to the Balitsky-Kovchegov equation in the large N_c limit.

4 Rapidity gaps at high- t

So far, all the processes we have looked at are close to $t = 0$, i.e. the outgoing proton(s) do not receive a large transverse momentum. Let us now focus on the case the $-t \gg \Lambda^2$. In this case, the incoming proton will typically be shattered. It is thought that the largeness of the momentum transfer will allow us to utilise QCD perturbation theory and hence to test the relevance of BFKL dynamics in these processes.

4.1 Vector mesons

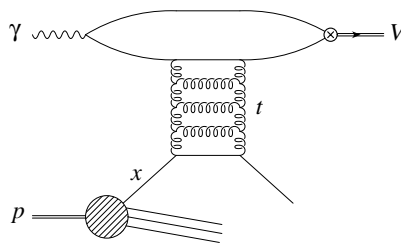


Fig. 8. High p_T vector meson production. (Figure from [30])

In Fig. 8 we show the diffractive production of a high p_T vector meson, V . The large momentum transfer across the gap, $-t \approx p_T^2$, almost always breaks up the proton and leads to a jet in the resultant debris. The non-perturbative dynamics is factorised into either the proton parton density functions or into the meson lightcone wavefunction, and QCD can be used to compute the dynamics of the exchange. The fact that $xW^2 \gg -t$ ensures that there is still a large rapidity gap between the proton dissociation products and the vector meson.

In leading order, BFKL predicts that the hard subprocess cross-section for scattering off quarks (gluons differ only by a colour factor) should go like [31]

$$\frac{d\sigma(\gamma q \rightarrow Vq)}{dt} \sim \frac{\alpha_s^4}{t^4} \frac{e^{8z \ln 2}}{z^{3/2}} \exp\left(-\frac{\ln^2 \tau}{112z\zeta(3)}\right), \quad (5)$$

where

$$\tau = \frac{-t}{Q^2 + m_V^2} \quad \text{and} \quad z = \frac{3\alpha_s}{2\pi} \ln \frac{xW^2}{s_0}.$$

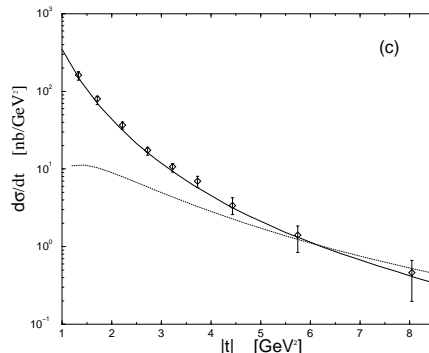


Fig. 9. Comparison of data [32] with theory for high p_T ρ production. The solid line is LO BFKL and the dotted line two-gluon exchange. (Figure from [33])

Comparison of the leading order BFKL calculation with the ZEUS data is shown in Fig. 9 [33]. The calculation is a fit to the data with $s_0 = \beta m_V^2 - \gamma t$ and α_s being the free parameters. The fit shown corresponds to $\beta = 0$, $\gamma = 1$ and $\alpha_s = 0.20$. Good agreement is also found (with the same parameters) with the data on the ϕ and J/ψ mesons [33]. Note that it is not possible to get good agreement in the approximation that only two-gluons are exchanged between the diquark system and the struck parton.

The above curves were computed assuming a very simple form for the meson wavefunction. In particular, it is assumed that the quarks share equally the momentum of the meson. Relativistic corrections to this simple approximation have been considered [29] and do not appear to spoil the good agreement [30]. Inclusion of relativistic corrections also allows one to quantify the degree to which the helicity of the meson differs from that of the photon, and comparison with data is once again encouraging [30].

In the future, data will become available on high- t photon production. This is something to look forward to, since it avoids the uncertainty associated with the production of the vector meson.

4.2 Gaps between jets

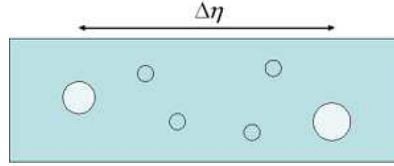


Fig. 10. Dijet production with a rapidity gap

As well as vector meson production, one can look for rapidity gaps between jets in photon-hadron and hadron-hadron collisions [34]. The typical final state topology is shown in Fig. 10, where two jets are produced far apart in rapidity and there is a gap between the jets. Early measurements at HERA [35] and the Tevatron [36,37] have been compared to theory and leading order BFKL does fine [38,39]. However, conclusive statements are hard to make either because the gap is not large enough (i.e. the excess over non-BFKL QCD is small) or hadronisation corrections are large [38].

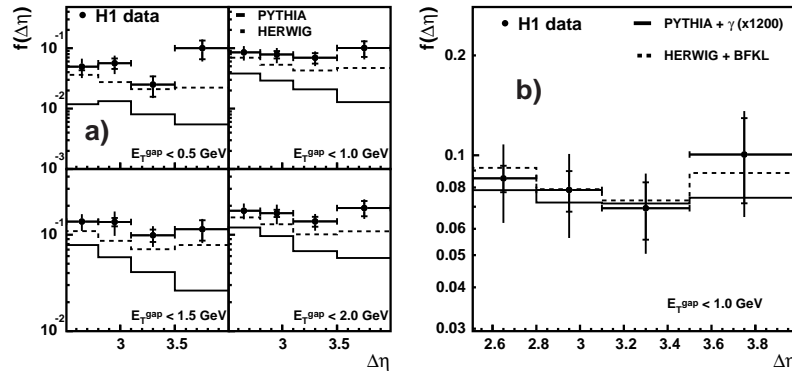


Fig. 11. Recent H1 results on gaps between jets shown as a function of rapidity gap and transverse energy between the jets. (Figure from [40])

There has been significant recent progress, both experimentally and theoretically in this area which has to some extent shifted interest away from BFKL dynamics and into the domain of jet energy flows. H1 has focussed on the definition of the gap. They use the k_T cluster algorithm to put all hadrons

into jets, after which they select the two highest p_T jets. The summed transverse energy between these two jets (E_T^{gap}) is then used to define a gap. As can be seen in Fig. 11, for low E_T^{gap} , one can really speak of a rapidity gap and a very clear excess is seen in the data over the standard Monte Carlos, whilst at larger values of E_T^{gap} the enhancement is less pronounced [40]. By defining their gaps this way, H1 has reduced its sensitivity to soft gluon radiation by effectively cleaning up the edge of the gap in a way which makes possible direct comparison with future theoretical calculations.

On the theoretical side, Dasgupta & Salam have recently pointed out that there is a previously unconsidered mechanism which ought to be considered when considered interjet energy flows [41]. In particular, they have discovered a class of “non-global” logarithms which ought to be summed at the single logarithm level.

5 Summary

The key conclusions of this talk can be summarised as follows:

- Regge factorisation and QCD evolution work well to describe diffractive deep inelastic scattering at HERA
- HERA partons may well be useful at the Tevatron provided one accounts for gap survival at a level of around 10%. Tevatron measurements at lower x_F would help.
- There is a need to measure exclusive central dijet production at Tevatron Run II in order to constrain diffractive higgs cross-sections at the LHC.
- Position on saturation is not clear. Ideally one would like to go to lower x .
- High- t vector meson production is well described by leading order BFKL.

Acknowledgements

Special thanks to Brian Cox, Rikard Enberg and Paul Newman for their help in preparing this talk. Thanks also to the conference organisers for their invitation to participate.

References

1. T. Affolder et al, CDF Collaboration: Phys. Rev. Lett. **85**, 4215 (2000).
2. C. Adloff et al, H1 Collaboration: Z. Phys. C **76**, 613 (1997).
3. J. Breitweg et al, ZEUS Collaboration, Eur. Phys. J. C **6**, 43 (1999).
4. P. Thompson: ‘Jets and E_t flows in diffraction at HERA’, talk presented at DIS 2002, April-May 2002, Acta Phys. Polon B **33**, 3213 (2002).
5. F.-P. Schilling: ‘Measurement and NLO DGLAP QCD Interpretation of Diffractive DIS at HERA’, talk presented at DIS 2002, April-May 2002, Acta Phys. Polon B **33**, 3511 (2002).

6. S. Schätzel, ‘Diffractive final states at HERA’, talk presented at the Workshop on Low x Physics, Antwerpen, September 2002.
7. J.C. Collins: ‘Factorization in hard diffraction’, talk presented at the Ringberg Workshop, J. Phys. G **28**, 1069 (2002), and references therein.
8. E. Gotsman, E. Levin, U. Maor: Phys. Rev. D **60**, 094011 (1999); A. Kaidalov, V.A. Khoze, A.D. Martin, M.G. Ryskin: Eur. Phys. J. C **21**, 521 (2001).
9. L. Alvero, J.C. Collins, J. Teron, J.J. Whitmore: Phys. Rev. D **59**, 074022 (1999); talk presented at DIS 1998, April 1998; L. Alvero, J.C. Collins, J.J. Whitmore: Nucl. Phys. Proc. Suppl. **79**, 382 (1999).
10. F. Abe et al, CDF Collaboration: Phys. Rev. Lett. **78**, 2698 (1997).
11. F. Abe et al, CDF Collaboration: Phys. Rev. Lett. **79**, 2636 (1997).
12. T. Affolder et al, CDF Collaboration: Phys. Rev. Lett. **84**, 5043 (2000); T. Acosta et al, CDF Collaboration: Phys. Rev. Lett. **88**, 151802 (2002).
13. B. Abbott et al, D0 Collaboration: Phys. Lett. B **531**, 52 (2002).
14. T. Affolder et al, CDF Collaboration: Phys. Rev. Lett. **84**, 232 (2000).
15. R. Appleby, J.R. Forshaw: Phys. Lett. B **541**, 108 (2002).
16. B.E. Cox, J.R. Forshaw: Comput. Phys. Commun. **144**, 104 (2002); www.pomwig.com.
17. A. Schäfer, O. Nachtmann, R. Schöpf: Phys. Lett. B **249**, 331 (1990); A. Bialas, P.V. Landshoff, Phys. Lett. B **256**, 540 (1991); Yu. L. Dokshitzer, V.A. Khoze, T. Sjöstrand: Phys. Lett. B **274**, 116 (1992); J.D. Björken: Phys. Rev. D **47**, 101 (1993).
18. V.A. Khoze, A.D. Martin, M.G. Ryskin: ‘Diffractive Higgs Production: Myths and Reality’, hep-ph/0207313; Eur. Phys. J. C **14**, 525 (2000).
19. A. de Roeck, V.A. Khoze, A.D. Martin, R. Orava, M.G. Ryskin: Eur. Phys. J. C **25**, 391 (2002).
20. N.N. Nikolaev, B.G. Zakharov: Z. Phys. C **53**, 331 (1992); B.Z. Kopeliovich, J. Nemchik, N.N. Nikolaev, B.G. Zakharov: Phys. Lett. B **309**, 179 (1993); N.N. Nikolaev, B.G. Zakharov: Z. Phys. C **64**, 631 (1994); J. Nemchik, N.N. Nikolaev, E. Predazzi, B.G. Zakharov: Z. Phys. C **75**, 71 (1997).
21. K. Golec-Biernat, M. Wüsthoff: Phys. Rev. D **60**, 114023 (1999); Eur. Phys. J. C **60**, 313 (2001).
22. J. Bartels, K. Golec-Biernat, H. Kowalski: Phys. Rev. D **66**, 014001 (2002).
23. J.R. Forshaw, G. Kerley, G. Shaw: Phys. Rev. D **60**, 074012 (1999).
24. J.R. Forshaw, G. Kerley, G. Shaw: Nucl. Phys. A. **675**, 80c (2000).
25. M.F. McDermott, R. Sandapen, G. Shaw: Eur. Phys. J. C **22**, 655 (2002).
26. L.V. Gribov, E.M. Levin, M.G. Ryskin: Phys. Rep. **100**, 1 (1983).
27. Ia. Balitsky: Nucl. Phys. B **463**, 99 (1996); Yu. Kovchegov: Phys. Rev. D **60**, 034008 (2000); *ibid* D **61**, 074018 (2000).
28. see E. Iancu: ‘The Colour Glass Condensate’, plenary talk at Quark Matter 2002, July 2002, hep-ph/0210236, and references therein.
29. D.Yu. Ivanov, R. Kirschner, A. Schäfer, L. Szymanowski: Phys. Lett. B **478**, 101 (2000); erratum *ibid* B **498**, 295 (2001).
30. R. Enberg, L. Motyka, G. Poludniowski: talk presented at DIS 2002, Cracow, Poland, April-May 2002, Acta Phys. Polon B **33**, 3511 (2002).
31. J.R. Forshaw, M. Ryskin: Z. Phys. C **68**, 137 (1995).
32. S. Chekanov et al, ZEUS Collaboration: DESY-02-072, to be published in Eur. Phys. J. C.
33. J.R. Forshaw, G. Poludniowski: hep-ph/0107068, to be published in Eur. Phys. J. C.

- 34. A.H. Mueller, W.-K. Tang: Phys. Lett. B **284**, 123 (1992).
- 35. M. Derrick et al, ZEUS collaboration: Phys. Lett. B **369**, 55 (1996).
- 36. F. Abe et al, CDF Collaboration: Phys. Rev. Lett. **74**, 855 (1995); ibid **80**, 1156 (1998); ibid **81**, 5278 (1998).
- 37. S. Abachi et al, D0 Collaboration: Phys. Rev. Lett. **76**, 734 (1996); ibid **84**, 5722 (2000).
- 38. B.E. Cox, J.R. Forshaw, L. Lönnblad: JHEP 9910:023 (1999).
- 39. R. Enberg, G. Ingelman, L. Motyka: Phys. Lett. B **524**, 273 (2002).
- 40. C. Adloff et al, H1 collaboration: Eur. Phys. J. C **24**, 517 (2002).
- 41. M. Dasgupta, G. Salam: JHEP 0203:017 (2002).